Preferred citation: H. Eloranta and P. Saarenrinne. The Structure of Turbulence in the Near-wall Area of a Channel Flow". In **The science of papermaking**, *Trans. of the XIIth Fund. Res. Symp. Oxford, 2001*, (C.F. Baker, ed.), pp 605–618, FRC, Manchester, 2018. DOI: 10.15376/frc.2001.1.605.

THE STRUCTURE OF TURBULENCE IN THE NEAR-WALL AREA OF A CHANNEL FLOW

H. Eloranta and P. Saarenrinne

Energy and Process Engineering, Tampere University of Technology,
P.O. BOX 589, FIN - 33101 Tampere, Finland

ABSTRACT

Fluid dynamics plays an essential role in the paper manufacturing process. The quality of paper is affected by the turbulence properties in the headbox and jet. In this paper the structure of turbulence in the wall area of a two-dimensional converging channel is studied experimentally. The measurements are performed with Particle Image Velocimetry, which provides instantaneous two-dimensional velocity fields. The structure of turbulence is studied by analysing both instantaneous and time-mean velocity fields. As a result several kind of flow structures can be identified close to the channel walls. The most prominent are streamwise elongated structures, which manifest themselves as a spatial modulation of the streamwise velocity component. Substantial activity in the near-wall region is related to the mean-shear close to the surface. The mechanisms of the wall-turbulence are discussed in a short review of the main concepts found in the literature. The results of this study are expected to improve the understanding of the significance of the headbox slice boundary layers in the papermaking process.

1 INTRODUCTION

The quality of the sheet is characterised by a multitude of different properties such as basis weight profiles and fibre orientation. Most of these properties are suggested to have a fluid mechanical origin in the headbox, even if the connection to the flow phenomena is indistinct. The flow in the headbox is a combination of several processes and phenomena with strong interactions. To guarantee a high sheet quality, the headbox has to generate and sustain a certain level of turbulence to prevent the flocculation of fibres. Furthermore, a disturbance-free jet without secondary flows, wakes and other non-uniformities is desirable because any unevenness in the flow field can affect the quality of the final sheet. Besides steady and homogeneous flow, the jet speed and impingement geometry must be controlled accurately. Disturbances initiated at any stage in the headbox may transfer with the flow and in the absence of damping effects even increase in strength. Potential sources of disturbances are, for example, the tubebank, boundary layers, trailing-edges of the vanes and slicebar. The headbox fluid dynamics and disturbances initiated by different sources is studied by several authors, see e.g. [1,2,3].

The flow in the headbox slice chamber is bounded by converging walls, which strongly affect the flow dynamics. The action of viscosity retards the motion of the fluid near a surface and consequently decreases the momentum of the fluid. The zone, where this phenomenon of viscosity dominates, is called the boundary layer. The innermost part of this layer close to the surface is a significant source of turbulent kinetic energy production. It is also the origin of mechanisms, which give rise to the large-scale coherent flow structures that appear throughout the boundary layer. The nature of the boundary layer varies considerably as a function of the Reynolds number and many other conditions. The focus of this study are the coherent flow structures evolving in the boundary layers originating from the instability mechanism in the near-wall turbulence and main-stream. The strength and spatial scales of these structures is examined in detail at various positions along the test channel. This information provides some characteristics of the boundary layers and their development to the downstream direction in a converging channel.

2 BOUNDARY LAYERS AND COHERENT FLOW STRUCTURES

In the turbulent boundary layer kinetic energy of the free-stream is converted into turbulent fluctuations and then dissipated into internal energy. The process is discontinual, i.e., intermittent in the sense that rapid periods of active production are mixed with more quiescent phases in the cycle. Turbulent boundary layer can be divided into several layers according to the time-mean statistics. These layers are the viscous sublayer, buffer layer, logarithmic layer and outer layer. A lot of effort has been focused to understand the dynamics of the near-wall events and their interaction with the free-stream. The work was originally initiated by flow visualisations that showed the presence of coherent flow structures close to the surface. Despite the intensive work, many fundamental issues in the boundary layer dynamics still remain unknown, reflecting the complexity of the phenomena.

Even the definition of a coherent structure is disputed. For example, the following definition has been proposed [4]: "A coherent motion (structure) is defined as a three-dimensional region of the flow over which at least one fundamental flow variable (velocity component, density, temperature, etc.) exhibits a significant correlation with itself or with another variable over a range of space and/or time that is larger than the smallest local scales of the flow." The significance of coherent structures is their essential role in the generation of turbulence shear stress. Velocity fluctuations tend to occur intermittently with sharp spikes. These spikes are often in another order of magnitude than the average value and therefore responsible for the maintenance of turbulence. If the motions in the turbulent boundary layer were purely random without any intercorrelations between the velocity fluctuations, the shear stress would be zero. The fact that the innermost region of the boundary layer is the source of nearly all turbulent kinetic energy production in the wall-area points out that especially organised motions are present close to the wall.

The flow pattern within the innermost layers (i.e., the sublayer and lower-part of the buffer layer) is quite non-uniform with narrow, elongated regions of low momentum and relatively shorter and wider regions of high momentum. Thus, the flow has a kind of streaky appearance. The majority of the turbulence production in the entire turbulent boundary layer occurs in the buffer layer. The process involves violent outward motions of low-speed fluid (ejections) and inrushes of high-speed fluid directed towards the wall at a shallow angle (sweeps). The role of these spatial velocity modulations is commonly related to the shear between high- and low-speed fluid. Local shear-layers are supposed to be the source of instabilities inducing vortices and other flow structures in the layers above. The mechanism behind the ejections and sweeps is in general explained to be the "pumping" action of quasi-streamwise upward-tilted vortices conveying near-wall low-speed fluid away from the wall and correspondingly bringing high-speed fluid from the outer layers towards the wall (see Figure 1). The vortices responsible for the

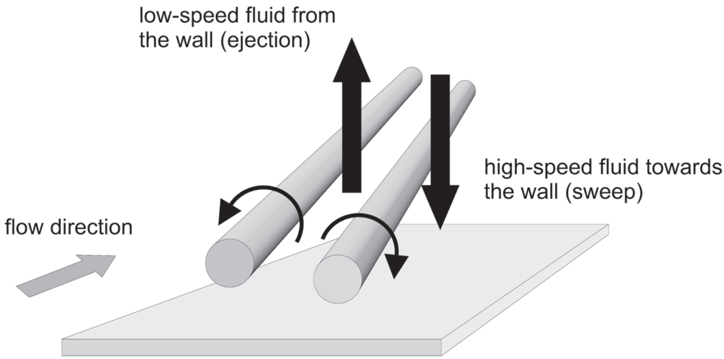

Figure 1 A pair of quasi-streamwise vortex tubes conveys high-speed fluid towards the wall and low-speed fluid away from the wall.

wall-normal transport of momentum are observed to have a varying degree of stretching and symmetry.

The dissipation rate in the outer layer is greater than the turbulence kinetic energy production. Therefore, the energy is necessarily convected from the near-wall area outwards to maintain the outer-layer turbulence. The energy is transferred both directly (through mass transfer from the ejections and sweeps) and indirectly (outward growth of vortical structures). Large-scale coherent motions extending to the outer part of the boundary layer are evident from many studies: see e.g., [5,6,7 and 8]. The flow structures in the outer layer are also distinctly elongated in the streamwise direction. The scale of these structures in the streamwise direction can be several times larger than the local boundary layer thickness differing significantly from the scale of the widely studied structures in the viscous sublayer and buffer layer.

Near-wall turbulence production is generally considered to be a self-sustaining cycle with outer flow structures having a definite but not controlling effect on the near-wall events through the entrainment. Complicated interaction between the outer and inner layer appears to be important since the extremely small-scale events in the near-wall area cannot directly be responsible for the large-scale structure in the outer-layer. Various authors propose that the low-momentum structures in the outer layer are induced by packets of hairpin-like vortices aligned in the streamwise direction. This mechanism is similar to the one suggested to be responsible for the near-wall ejections and sweeps. However, the merging of several vortices can create structures extending throughout the boundary layer combining strength greater than any individual vortex loop. The wall-turbulence is proposed to be maintained by a cycle in which streamwise vortices extract energy from the mean-flow to create alternating regions of high- and low-momentum fluid [9]. Local shear-layers between these regions in turn give rise to vortices created presumably through inflectional instabilities. A similar interpretation is suggested in [10], where it is stated that "The vortex roll-up is frequently caused by time-dependent interactions where high-speed flow shears over a region of low-speed fluid, creating one or more horseshoe or arch-like vortices. The horseshoe vortices induce low-speed fluid under their arches. This induced low-speed fluid can form a shear layer with up-stream high-speed fluid, forming another arch." Although most structural features are evident from experiments and DNS databases, the dynamical relationship of events is still poorly understood. A discussion, review and list of further literature are provided e.g., in [4 and 11].

3 EXPERIMENTS

The measurements are carried out in a two-dimensional convergent channel made of plexiglas. The geometry of the channel is presented in Figure 2. All dimensions are normalised by the height of the channel at the end of the convergent section (H). The channel width, i.e., the spanwise dimension, is 34 H. The channel is ran with pure water. The Reynolds number used in the measurements is 77000, based on the channel half height. In the experiments Digital Particle Image Velocimetry (DPIV) is used to measure instantaneous two-dimensional velocity fields close to the channel walls. Measurements are performed in five streamwise stations, labeled A . . . D. At each station, several planes parallel to the surface at different distances from the wall are measured. At each distance a set of 300 velocity fields is gathered. In

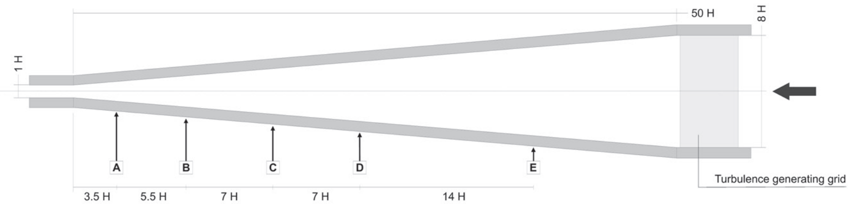

Figure 2 Geometry of the convergent channel.

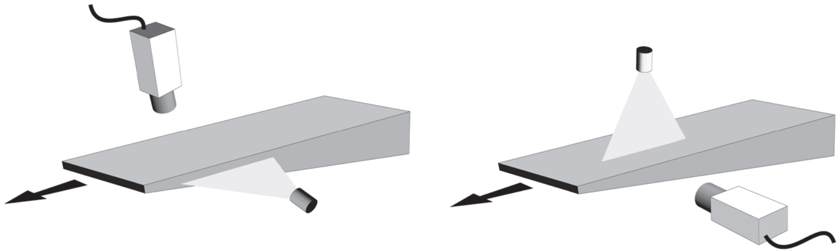

Figure 3 The arrangement of the laser and the camera in the experiments. Set-up to measure streamwise-spanwise -plane on the left and streamwise-wall normal -plane on the right.

addition, one set of data in the wall-normal plane is measured at each station. In this plane, each set contains 500 velocity fields.

In DPIV the flow is seeded by tracer particles and the area of interest is illuminated by a thin sheet of light. The illumination is provided by two short-duration laser pulses with an accurately adjusted time-separation. Synchronised to each of the pulses, the light scattered by the tracer particles is recorded by a high resolution CCD-camera. Two consecutively exposed images are then stored as a double-frame image. The temporal resolution of the system is limited to about 4 Hz. A picture of the experimental set-up with the laser and CCD-camera of the PIV-system is presented in Figure 3.

As a first step in evaluating the velocity field from a double-frame image, the image is divided into interrogation areas. The average particle displacement between the two frames in each interrogation area is calculated by cross-correlation analysis. The highest peak in the correlation plane corresponds to the average displacement of the punch of particles in the specific interrogation area. Since the time separation between the two frames is known, the velocity of the particles can be solved. When the cross-correlation analysis for each interrogation area of the image domain is performed, the velocity field of the entire image area can be presented. By using the overlap of 50% for the interrogation areas, a virtually better resolution is achieved.

4 TOOLS FOR DATA ANALYSIS

Instantaneous velocity vector fields contain a lot of information of the structure and properties of the flow. Visual examination of a sample of instantaneous fields can provide a rough picture of the flow pattern and phenomena. Computation of the time-mean turbulence quantities yields average velocity, turbulence intensity and turbulence kinetic energy. These quantities characterise the time-mean properties of the flow. The formulas for these quantities are following: average velocity (1), turbulence intensity (2) and turbulence kinetic energy (3):

$$U = \frac{1}{N}\sum_{\xi=1}^{N} u^{(\xi)} \tag{1}$$

$$TI = \frac{\sqrt{\overline{u'^2}}}{U} \tag{2}$$

$$k = \frac{1}{2}\left(\overline{u_x'^2} + \overline{u_x'^2}\right) \tag{3}$$

Here only two velocity components are taken into account. The third velocity component (i.e., normal to the measurement plane) is unavailable from the measurements and thus neglected. Symbol ξ corresponds to the index of the field in the measurement set.

Coherent flow structures are instantaneous in nature and the methods to detect these phenomena cannot utilise this kind of averaging procedure. One of the most powerful tools to characterise instantaneous flow structures is the space-correlation function. This function produces a correlation plane that portrays average spatial scales of the flow. The general formula for the second-order correlation can be written as:

$$\overline{\Phi_1'\Phi_2'} = R \cdot \Phi_{1,rms}\Phi_{2,rms} \tag{4}$$

Here Φ_1 and Φ_2 are two signals, corresponding now to velocities u_x and u_y. R is the correlation coefficient, which characterises the mean kinematic structure of turbulence independent of the fluctuations magnitude. If $\Phi_1 = \Phi_2$, the function is called direct- or auto-correlation. In the following auto-correlation function for the streamwise velocity component is computed. Considering the x-component as the streamwise component, the auto-correlation function can be written as:

$$R^{(\xi)}(\Delta r) = \frac{1}{n}\sum_{i=1}^{p}\sum_{j=1}^{q}\left(\frac{u_x'(r(i,j),\xi)\cdot u_x'(r(i,j)+\Delta r,\xi)}{u_{x,rms}(r(i,j))\cdot u_{x,rms}(r(i,j)+\Delta r)}\right) \tag{5}$$

As the location r with all correlation lags Δr moves over the domain (size pxq), it yields a two-dimensional correlation plain. A set of N two-dimensional vector fields can be analysed one by one and finally the averaged correlation function can be found by summation:

$$R_{avg}(\Delta r) = \frac{1}{N}\sum_{\xi=1}^{N} R^{(\xi)}(\Delta r) \tag{6}$$

By means of the correlation function, some important length scales of turbulence are defined. The integral length scale, which is a measure of the average spatial extent of coherent structures appearing in the velocity fluctuations, is defined as:

$$\Gamma = \int_0^{\infty} R(\Delta r)d(\Delta r) \tag{7}$$

5 RESULTS

The influence of the wall penetrates to the bypassing fluid a distance at least that of the local boundary layer thickness. At the outer edge of the boundary layer the velocity reaches the main-stream value. This causes the mean-shear to vanish, which suppresses the turbulence production. Averaged velocity profiles normalised by the mean-velocity at the channel exit in all measurement stations along the channel are presented in Figure 4. The profiles show a decrease in the boundary layer thickness to the downstream direction. The influence of the turbulence grid can be seen clearly in the first upstream profile (E). Here the flow is still under strong initial development, which can be observed from the shape of the profile. The maximum velocity is achieved far away from the wall. In the next position to the downstream (D) the profile is flatter and approaching the common profile of turbulent channel flow.

The boundary layer thickness, which is defined as the distance from the wall where the tangential velocity has reached 99% of the main-stream value, is presented in Figure 5. High value in the first position is the result of the undeveloped velocity profile and therefore not directly related to the boundary layer. After the initial development, the boundary layer thickness reaches a value of about 0.4 H at the position D. After this the boundary layer thickness decreases quite linear to the exit. In the same figure is also presented the turbulence intensity at the wall-normal distance 0 H. The distance 0 H

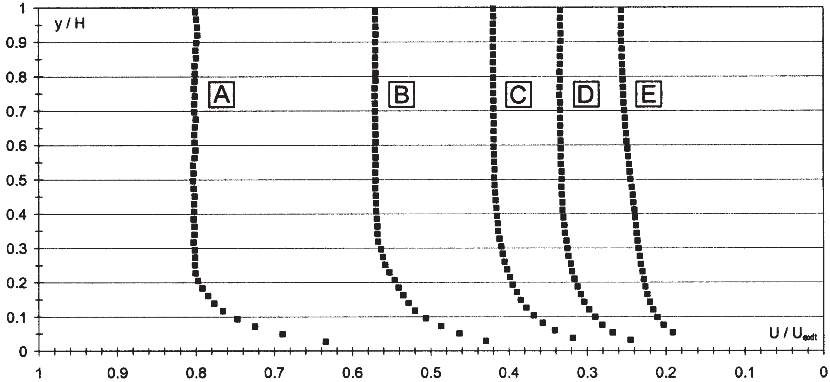

Figure 4 Wall-normal velocity profiles at all measurement stations.

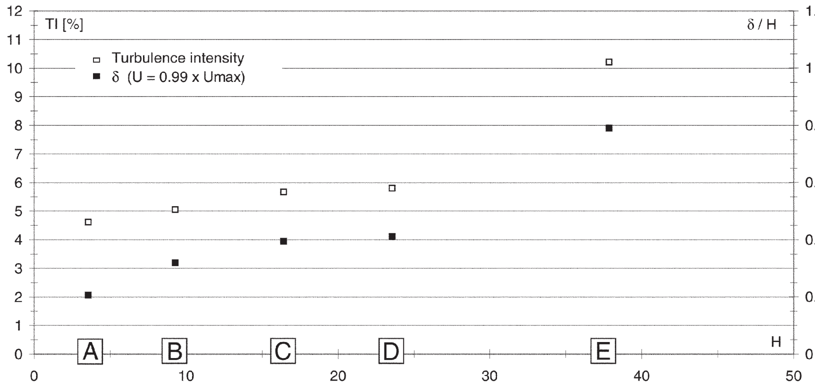

Figure 5 Streamwise profiles of the turbulence intensity and boundary layer thickness.

refers to the measurement plane right next to the wall. In the beginning of the channel the level of turbulence intensity undergoes a rapid drop. This is due to increasing mean velocity and the decay of the grid-turbulence. After station D the decrease is more moderate.

The structure of the flow in the streamwise-spanwise -plane is examined in the following by means of the Reynolds decomposition. In this

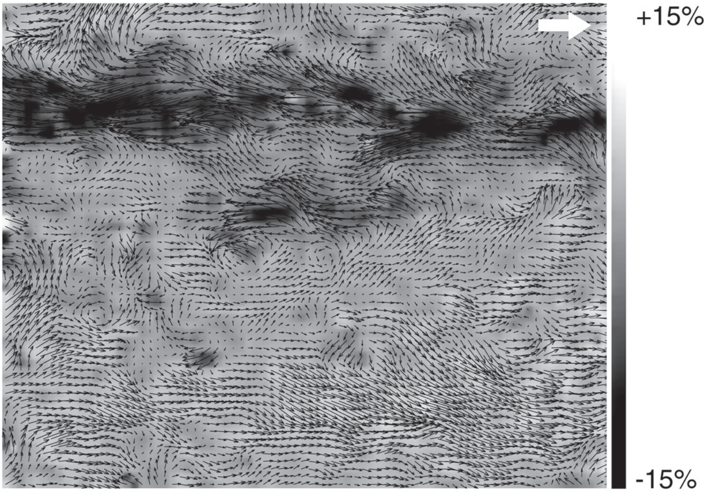

Figure 6 Velocity fluctuation field in the positon D, at the distance 0.07 H from the channel surface. Contours on the background represent the magnitude of the streamwise component.

decomposition the ensemble-averaged velocity field is subtracted from an instantaneous field. Figure 6 measured in the position D at the distance 0.07 H from the surface gives an example of the structure of the velocity fluctuation field close to the wall. The white arrow points to the streamwise direction. The vectors represent both the streamwise and spanwise components of the velocity fluctuation and the contours on the background only the magnitude of the streamwise component. The scale of the contours corresponds to the magnitude of fluctuation in respect to the time-mean value. Thus, negative values indicate low momentum. The flow field is dominated by large-scale high- and low-momentum structures. These structures are distinctly elongated in the streamwise direction and manifest themselves particularly in the streamwise velocity component. The contours of the spanwise component do not show the same degree of coherence. Furthermore, these structures are intermittent and purely random in nature. As a set of instantaneous fields is ensemble-averaged all structures vanish and an even velocity field is obtained. In addition to these streamwise elongated regions, other coherent structures can be detected from instantaneous fields including vortices having their axis normal to the measurement plane and sink-like points generated by the flows three-dimensionality.

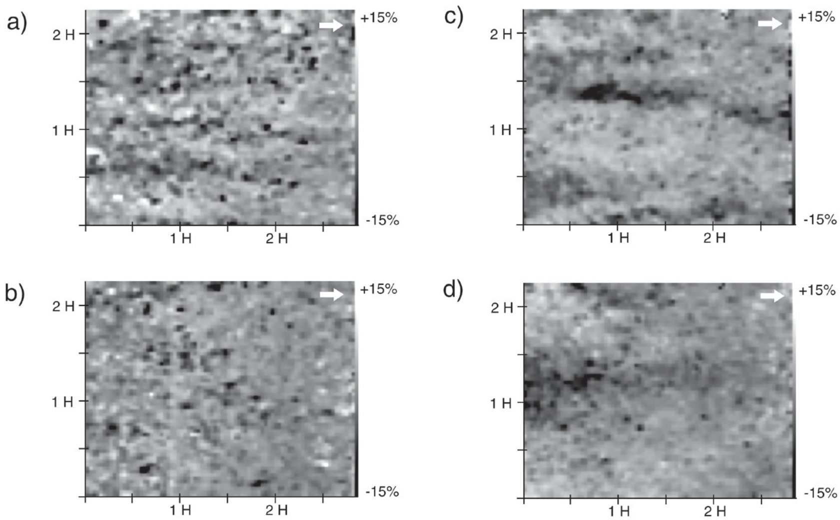

Figure 7 Contours of the streamwise velocity fluctuation component. a) position A, at the surface, b) pos. A, at the distance 0.07 H form surface, c) pos. C, distance 0.07 H, d) pos. C, distance 0.21 H.

Some other examples of instantaneous fluctuation fields are presented in Figure 7. Here, again the contours represent the magnitude of the streamwise velocity fluctuation and the white arrow points to the streamwise direction. Figures 7 a and b present the flow field in the position A at distances 0 and 0.07 H, respectively. At the distance 0 H the flow shows a slightly streamwise elongated structure. At the distance 0.07 H, which is in the outer part of the boundary layer, the flow field is more homogeneous. Figures 7 c and d represent the flow field in the position C at distances 0.07 and 0.21 H, respectively. At this station high- and low-momentum structures are pronounced at the distance 0.07 H. Further away from the wall, at the distance 0.21 H, the structures are weaker but show larger scales especially in the spanwise direction than in the wall proximity.

Figure 8 presents the correlation coefficient maps at the wall-normal distances 0.07 and 0.21 H in each station. The correlation function confirms the observations made from individual velocity fluctuation fields. Correlation maps show that streamwise elongated flow structures are characteristic. The black arrow points to the streamwise direction. It has to be emphasised that these fixed wall-distances are not consistent in the sense that the boundary

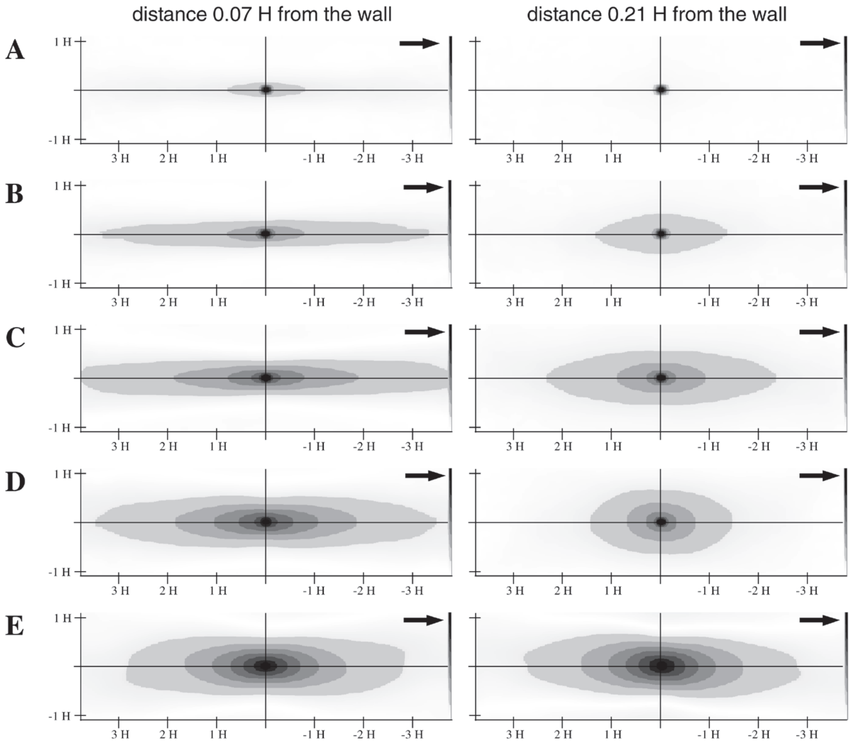

Figure 8 Two-dimensional correlation maps for the streamwise velocity fluctuation. Left column presents correlation maps at the distance 0.07 H form the wall in all streamwise stations (A . . . E) and right column at the distance 0.21 H in the same stations.

layer thickness is decreasing to the downstream and thus the measurement planes move outwards in the wall-coordinates. In the last downstream station the boundary layer is thin, resulting in insufficient measurement resolution to reveal the structures extremely close to the wall. Thus, the disappearance of coherent structures in the downstream stations is partially a consequence of the decrease in the boundary layer thickness, which confines the structures closer to the wall. These correlation maps should be examined, together with Figure 9, which presents the turbulence kinetic energy. Minimum level of turbulence kinetic energy is located at the stations C and D. To the downstream direction, the turbulence kinetic energy is increasing again due to the

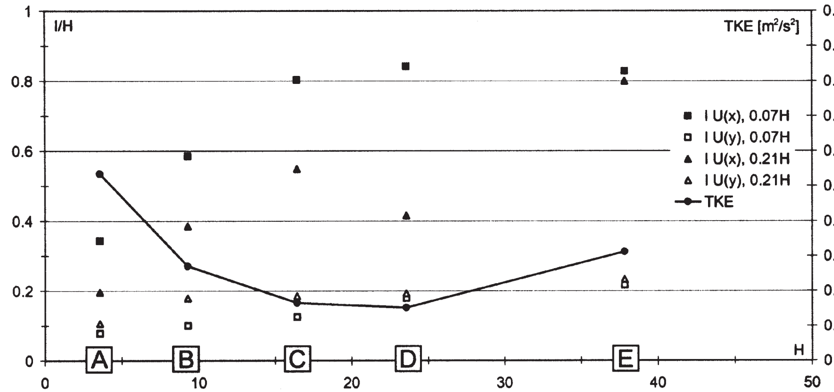

Figure 9 Integral length scales for the streamwise velocity component in the streamwise and spanwise direction at distances 0.07 and 0.21 H from the wall.

acceleration. The turbulence kinetic energy reveals the power connected to the coherent structures. Minimum turbulence energy coincides with widest spatial scales. At the station A, the turbulence kinetic energy is high, but it is concentrated on small scales. In Figure 9 is also presented the integral length scales in the streamwise and spanwise directions corresponding to the correlation maps presented in Figure 8. There is a remarkable decrease in the average streamwise scales to the downstream direction, which is obvious from Figure 9 as well. The integral length scale in the streamwise direction drops from the value 0.8 down to 0.3. For the spanwise scales the value drops from 0.2 to 0.1. Between the positions E and D the streamwise length scale at the distance 0.21 H shows a rapid decrease. This is interpreted as the result of the decay of grid-turbulence, which is more dominating further away from the wall. Between the positions D and C the integral length scale is increasing again, which shows that the boundary layer is still developing intensively. Only in the three last positions is a clear decrease in the streamwise scales due to the acceleration observed.

6 CONCLUSIONS

PIV-technique was able to reveal much about the nature of wall-turbulence in a convergent channel. The velocity fluctuations are highly unisotropic in the wall region, whereas the state of the main-flow is more homogeneous and isotropic. The turbulence kinetic energy is predominantly associated with the fluctuations in the streamwise velocity component. Organised motions throughout the boundary layer are evident. Characteristic structures are in the streamwise direction elongated regions of uniform momentum. The scale of these structures varies considerably in the streamwise direction due to the channel geometry and natural development of the boundary layers. The scale and magnitude varies also in the wall-normal direction. Widest scales are observed in the outer layer, whereas the maximum of the turbulence kinetic energy is found in the inner layers close to the wall.

REFERENCES

1. Aidun, C.K., "A fundamental opportunity to improve paper forming", *Tappi J.*, **79**(6): pp. 55–60 (1996).
2. Parsheh, M., "Aspects of boundary layers, turbulence and mixing in a plane contraction with elastic vanes, envisaging potential application to paper manufacturing", Licentiate thesis. Royal Inst. of Technology, FaxénLaboratoriet, Stockholm, Sweden (1999).
3. Söderberg, D., "Hydrodynamics of a plane liquid jets aimed at applications in paper manufacturing", Doctoral thesis. Royal Inst. of Technology, Faxén-Laboratoriet, Stockholm, Sweden (1999).
4. Robinsson, S. K., "Coherent motions in the turbulent boundary layer", *Annu. Rev. Fluid Mech.*, 23, pp. 601–639 (1991).
5. Blackwelder, R. F. and Kovasznay, L. S. G., "Time scales and correlations in turbulent boundary layer", *Phys. Fluids*, **15**(9), pp. 1545–1554 (1972).
6. Wark, C. E. and Nagib, H. M., "Experimental investigation of coherent structures in turbulent boundary layers", *J. Fluid Mech.*, 230, pp. 182–208 (1991).
7. Kähler, C. J., Adrian, R. J. and Willert, C. E., "Turbulent boundary layer investigations with conventional-and stereoscopic particle image velocimetry", Proceedings of the 9th International Symposium on Applications of Laser Techniques to Fluid Mechanics, Portugal, July 13th-16th (1998).
8. Tomkins, C. D. and Ardian, R. J., "Characteristics of vortex packets in wall turbulence. Proc. Turbulence and Shear Flow Phenomena – 1, First International Symposium", ed. Banerjee, S. and Eaton K., California, USA, September 12th-15th, pp. 31–36 (1999).
9. Jimenez, J. and Pinelli, A., "Dynamics of the structures of near-wall turbulence. In Simulation and Identification of organized structures in flows", ed. Sørensen et. al., Kluwer Academics (1998).
10. Meinhart, C. D. and Adrian, R. J., "On the existence of uniform momentum zones in a turbulent boundary layer", *Phys. Fluids A*, **4**(4): pp. 694–696 (1995).
11. Bogart, D. G. and Thole, K. A, "Coherent Structures", in *The Handbook of Fluid Dynamics*, ed. R. W. Johnson, CRC Press LCC (1998).

Transcription of Discussion

THE STRUCTURE OF TURBULENCE IN THE NEAR-WALL AREA OF A CHANNEL FLOW

H. Eloranta and P. Saarenrinne

Tampere University of Technology

Peter Herdman Arjo Wiggins

I believe that the surface energy on the Perspex and its interface with the water have some considerable effect on the local turbulence, have you tried anything to make the surface specifically hydrophilic or hydrophobic and observe any changes?

Hannu Eloranta

No we haven't.